Oligomerization of a 45 Kilodalton Fragment of Diphtheria Toxin at pH 5.0 to a Molecule of 20−24 Subunits†

Charles E. Bell,‡ Pak H. Poon, Verne N. Schumaker, and David Eisenberg*

UCLA−DOE Lab of Structural Biology and Molecular Medicine, Molecular Biology Institute, and Department of Chemistry and Biochemistry, Box 951569, University of California at Los Angeles, Los Angeles, California 90095-1569

Received June 2, 1997; Revised Manuscript Received September 4, 1997⊗

ABSTRACT: Diphtheria toxin (DT) is a 58 kDa protein, secreted by lysogenic strains of *Corynebacterium diphtheriae*, that causes the disease diphtheria in humans. The catalytic (C) domain of DT kills host cells by gaining entry into the cytoplasm and inhibiting protein synthesis. The translocation of the C domain across the endosomal membrane and into the cytoplasm of a host cell is mediated by the translocation (T) domain of DT. This process is triggered by acidification from pH ∼7 to pH ∼5 within the endosome. Here we show that crm45 (cross-reacting material of 45 kDa), a 45 kDa deletion mutant of DT which contains the C and T domains but lacks the C-terminal receptor-binding (R) domain, undergoes a transition from a monomer to a large oligomer upon acidification from pH 7.0 to pH 5.0. Dynamic light scattering analysis of crm45 at pH 5.0 results in a polydispersity value of only 8−17%, suggesting that the oligomer is uniformly sized. Using analytical ultracentrifugation, measurements of the sedimentation rate and diffusion coefficient of crm45 at pH 5.0 result in a molecular mass determination of 890 ± 40 kDa (20 ± 1 subunits) for the oligomer. Equilibrium sedimentation data on crm45 at pH 5.0 are best fit by a single species with a mass of 1000 ± 50 kDa (24 ± 1 subunits). These results reveal the pH-dependent formation of a uniformly sized, 20−24 subunit oligomer of the C and T domains of DT, in solution. Because the oligomer of crm45 forms at the pH of the acidified endosome, it could be relevant to the translocation of the C domain of DT across the endosomal membrane and into the cytoplasm of host cells. The possible relevance of this oligomer of crm45 to the membrane translocation of the C domain of DT correlates with earlier kinetic studies of DT intoxication of Vero cells, which inferred the transfer of ∼20 C domains of DT to the cytoplasm of host cells, in a single event.

Several bacterially secreted toxins, including diphtheria toxin (DT)[1] of *Corynebacterium diphtheriae*, anthrax toxin of *Bacillus anthracis*, tetanus toxin of *Clostridium tetani*, and botulinum toxin of *Clostridium botulinum*, possess the remarkable capability of translocating a protein domain with toxic activity across a membrane and into the cytoplasm of a host cell (*1*). The basic mechanism (or mechanisms) by which these toxins are able to accomplish protein translocation across membranes of their host cells is poorly understood.

DT is one of the best characterized of the membrane-translocating bacterial toxins. DT has three structural domains which each carry out a distinct step in the killing of a host cell. First, the C-terminal receptor-binding (R) domain, residues 386−535, binds to a cell surface receptor, identified as the heparin-binding epidermal growth factor-like precursor (*2*). This allows DT to enter cells through an endosome by the process of receptor-mediated endocytosis (*3*). In the endosome, a drop in pH from ∼7 to ∼5 triggers a conformational change in the translocation (T) domain of DT, residues 200−386 (*4*). At pH ∼5, the T domain exposes hydrophobic regions (*5*−*7*), inserts into the endosomal membrane (*8*), and mediates the translocation of the N-terminal catalytic (C) domain, residues 1−187, across the endosomal membrane and into the cytoplasm. Once inside the cytoplasm of a host cell, the C domain of DT inhibits protein synthesis by catalyzing the ADP-ribosylation of elongation factor 2 (*9*).

One of the most poorly understood aspects of DT intoxication is the mechanism by which the T domain is able to translocate the C domain across the endosomal membrane. A possible mechanism is suggested by electrophysiological studies which show that at pH ∼5, the T domain of DT can form ion channels across planar lipid bilayers (*10, 11*). Since mutations in the T domain that affect channel activity also affect translocation of the C domain (*12*), it is conceivable that the ion channels formed by the T domain are identical to, or closely related to, a hydrophilic pore through which an unfolded form of the C domain could traverse the hydrophobic lipid bilayer.

The crystal structure of DT (*13, 14*), determined at pH 7, has also provided clues to the mechanism of translocation. At pH 7, the T domain is formed by a bundle of nine α-helices (Figure 1) which bears some structural resemblance to the pore-forming colicins of *E. coli* (*15*) and also to human Bcl-x_L (*16*). The C-terminal helices 8 and 9 of the T domain, which are connected by an acidic loop, are more apolar than most helices of globular proteins and are mostly buried in

† This work was supported by NIH Grant GM31299, DOE Grant DE-FC03-87ER60615, and NSF Grant MCB 9420769.

* Author to whom correspondence should be addressed at the Department of Chemistry and Biochemistry, UCLA.

‡ Present address: Department of Biochemistry & Biophysics, University of Pennsylvania, School of Medicine, Philadelphia, PA 19104-6059.

⊗ Abstract published in *Advance ACS Abstracts,* November 15, 1997.

[1] Abbreviations: DT, diphtheria toxin; crm45, cross-reacting material of 45 kDa; C domain, catalytic domain of DT; T domain, translocation domain of DT; R domain, receptor-binding domain of DT; DLS, dynamic light scattering.

S0006-2960(97)01301-9 CCC: $14.00

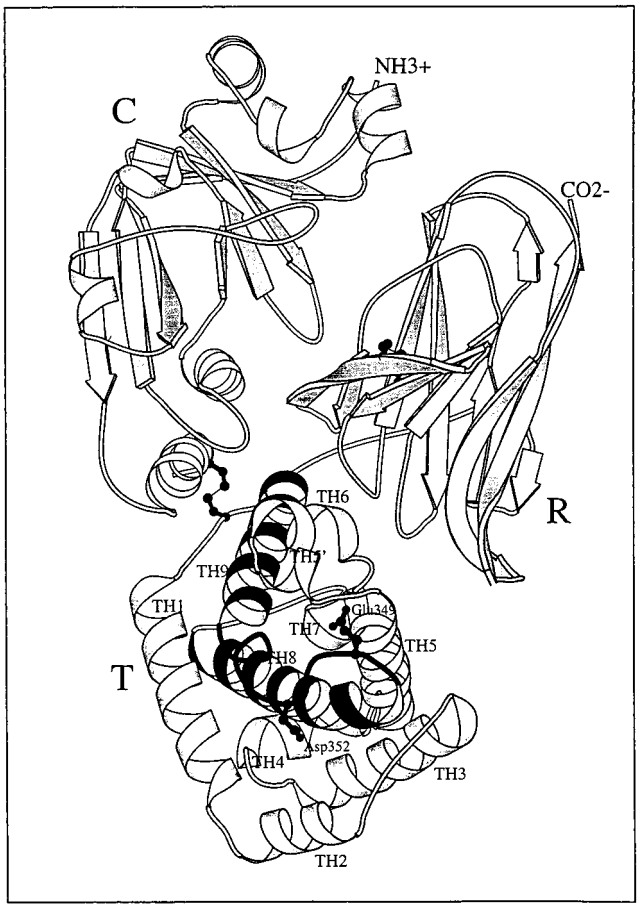

FIGURE 1: Crystal structure of monomeric DT at pH 7.0 [PDB code 1MDT (*14*)]. The catalytic (C) domain, residues 1−187, translocation (T) domain, residues 201−386, and receptor-binding (R) domain, residues 387−535, are shown in gray in ribbon representation. The secondary structures of the T domain (α-helices TH1−TH9) are labeled according to Bennett and Eisenberg (1994). The disulfide bond (Cys186−Cys201) linking the C and T domains is shown in black in ball-and-stick representation. The hydrophobic helical hairpin (TH8, TH9, and the loop that connects them), formed by residues 326−376 of the T domain, is highlighted in black. Two acidic residues of this hydrophobic hairpin, Asp352 and Glu349 on the loop connecting helices TH8 and TH9, are shown in black in ball-and-stick representation. Notice that helices TH8 and TH9 are mostly buried in the structure of the T domain at pH 7. Acidification could promote protonation of Glu349 and Asp352, making the TH8−TH9 helical hairpin more hydrophobic at low pH. Acidification is also believed to break the noncovalent interactions between the R domain and the C and T domains. The figure was prepared using MOLSCRIPT (*36*).

the structure, as are portions of helices 6 and 7. Based on this structure, it was proposed that acidification causes a conformational change in the T domain, starting with the separation of the R domain from the T and C domains. This exposes apolar portions of helices 6−9, leading to the insertion of helices 8 and 9 into the membrane. At pH 5, the acidic residues of the connecting loop could conceivably become protonated, making the helical hairpin more hydrophobic than at pH 7.

Mutational analyses further support the importance of the hydrophobic helical hairpin of the T domain. If one of the acidic residues in the loop connecting helices 8 and 9 is mutated to a positively charged lysine (Glu349 → Lys), the ion channel forming activity of the T domain is severely reduced (*17*). A recent study employing scanning cysteine mutagenesis, combined with electron paramagnetic resonance spectroscopy of nitroxide spin-labels, has provided strong evidence that helix 9 of the T domain is inserted across the membrane at low pH, with one side facing the hydrophobic interior of the lipid bilayer and the other side facing a hydrophilic pore (*18*).

Some evidence suggests that the membrane-bound, translocation-competent form of DT may be an oligomer. In a recent study, it was observed that a construct of the C and T domains of DT in which all but helices 8 and 9 of the T domain were deleted could form ion channels. This led to the conclusion that the construct must oligomerize in order to form a structure large enough to produce a channel across a lipid bilayer (*19*). In earlier studies of channel formation, it was observed that channel activity was nonlinearly dependent on toxin concentration. This led to the suggestion that the ion channel could be formed by an oligomer of DT (*10, 11*). The limited extent of hydrophobic sequence stretches within the T domain, as compared to typical membrane proteins, has led to the proposal that DT may oligomerize in order form a large enough hydrophobic surface area to interact with a lipid bilayer (*20*). Several other toxins, including anthrax toxin (*21*) and α-hemolysin (*22*), have been shown to convert from a water-soluble monomer to a membrane-soluble oligomer.

Despite this evidence, the formation of such an oligomer of DT at low pH, either in solution or in a lipid environment, has to our knowledge not been detected. The extensive aggregation of DT and the T domain at low pH has been observed and characterized by size-exclusion chromatography and native gel electrophoresis (*4, 6, 7*). This aggregation, however, has been attributed to contact between exposed hydrophobic sites on the T domain that would normally contact lipid.

In this study, we have characterized the low-pH solution properties of crm45 [cross-reacting material of 45 kDa (*23*)], a mutant form of DT that is truncated at Thr386 (*24*). Crm45 contains the C and T domains of DT but is missing the C-terminal 149 amino acids which comprise the R domain. Using dynamic light scattering (DLS), sedimentation velocity, and sedimentation equilibrium, we find that at pH 5, crm45 forms a uniformly sized oligomer of approximately 1000 kDa (∼24 subunits). Our results are consistent with the possibility that this oligomer of crm45, or a similar one formed by DT, could be relevant to the process by which the C domain of DT is translocated across the endosomal membrane and into the cytoplasm of a host cell.

MATERIALS AND METHODS

Crm45 Expression and Purification. Crm45 was expressed and secreted from the C7hm723(*β*-tox) M8 strain of *C. diphtheriae* (Dr. John R. Murphy, personal communication) in CY medium (*25*) as has been described (*26*). The cells were removed by centrifugation, and the supernatant was collected. After a cut at 50% saturated ammonium sulfate, crm45 was precipitated at 75% saturated ammonium sulfate, and collected by centrifugation. The precipitate was then dissolved in 0.01 M phosphate buffer, pH 7.2, and dialyzed against the same buffer. Crm45 was then purified by Poros HQ anion exchange perfusion chromatography, using a sodium chloride gradient elution. This purification step was done twice. Purified crm45 was then dialyzed back into 0.01 M phosphate, pH 7.2, and simultaneously concen-

Table 1: Dynamic Light Scattering Measurements of the Crm45 Fragment of DT and of Control Proteins To Estimate Molecular Masses and Extent of Aggregation; These Data Suggest That Crm45 Is a Monomer at pH 7.0 and a Fairly Monodisperse Oligomer of ~1100 kDa at Low pH[a]

molecule	pH	mg/mL	R_H (nm)[b]	molecular mass (kDa)	polyd (nM)[c]	% polyd[d]	baseline[e]	SOS_{error}[f]
crm45	7.0	1.0	3.1	46 ± 2	1.7	55	1.003	11.4
crm45	5.0	0.5	11.3	1029 ± 31	2.0	17	1.000	0.9
crm45	5.0	1.0	11.4	1056 ± 34	0.9	8	0.999	1.0
crm45	5.0	2.0	11.6	1100 ± 16	1.8	16	1.000	0.4
crm45	5.0	3.0	12.1	1235 ± 28	2.0	16	1.000	0.4
crm45	4.5	2.0	12.6	1347 ± 48	1.4	11	1.000	0.8
trypsin	−	2.0	2.3	22.8 ± 0.7	0.4	18	1.000	1.6
IgM	−	0.5	12.5	1322 ± 34	0.6	5	1.000	0.5

[a] All values represent the average of several measurements. [b] Mean hydrodynamic radius derived from the measured translational diffusion coefficient using the Stokes−Einstein equation. [c] Polydispersity value, indicating the standard deviation of the spread of particle sizes about the reported mean radius. [d] Polydispersity divided by the hydrodynamic radius. [e] Base line represents the completeness and fit of the regression. [f] Sum of squares measuring the closeness of fit between the experimental data and an autocorrelation function generated from the analysis results.

trated to 12 mg/mL (concentration determined by absorbance at 280 nm) using the Microprodicon dialyzer/concentrater. The final yield of crm45 was 50 mg per 2.4 L of cell culture.

Dynamic Light Scattering. All DLS measurements were performed using a DynaPro-801 Molecular Sizing Instrument (Protein Solutions, Inc., Charlottesville, VA). The AutoPro software package was used for all data analyses. In the DLS experiment, the sample protein solution, in a 7 μl flow cell, is illuminated by a 25 mW, 780 nm solid-state laser, and the intensity of light scattered at an angle of 90° is measured at intervals of approximately 4 μs by a solid-state avalanche photodiode. Using an autocorrelation function, the translational diffusion coefficient (D_T) of the sample particles in solution is evaluated by measuring the fluctuations in the intensity of the scattered light. The hydrodynamic radius (R_H) of the sample particles is derived from D_T using the Stokes−Einstein equation:

$$D_T = k_b T/6\pi\eta R_H$$

where k_b is Boltzmann's constant, T is the absolute temperature in degrees kelvin, and η is the solvent viscosity. The mass of the sample particles is estimated from R_H assuming that the particles are spherical and of standard density. Based on an attempt to fit the sizes of the sample particles to a monomodal distribution (one particle size), the polydisperisity, base line, and sum-of-squares parameters (see Table 1) give an indication of the homogeneity of particle sizes in the sample.

Soybean trypsin, molecular mass = 23 kDa, purchased from Sigma, in 150 mM NaCl, and pentameric IgM, molecular mass = 900 kDa (*27*), in 100 mM NaCl were used as standards. Crm45 and DT samples were prepared in 100 mM citrate, 150 mM NaCl at the pH and protein concentration indicated. All samples were 300 μL in volume and were filtered through 10 mm i.d., 0.1 μm Whatman Anatop inorganic membranes prior to analysis.

Sedimentation Velocity, Diffusion, and Sedimentation Equilibrium. All sedimentation experiments were performed at 15 °C. Sedimentation velocity measurements of crm45 in 100 mM citrate, 150 mM NaCl, pH 5.0 or 4.5 (Figure 2 and Table 2), were performed using a Beckman Model E analytical ultracentrifuge equipped with a UV optical system and a photoelectric scanner interfaced to an IBM PC. Sedimentation velocity and equilibrium measurements of crm45 in 15% sucrose, 100 mM citrate, and 150 mM NaCl, pH 5.0 (Figures 4 and 5), were performed using a Beckman Optima XL-A analytical ultracentrifuge. Sedimentation velocity experiments were performed at rotor speeds of 24 000, 36 000, or 56 000 rpm. *s*-rates were determined from the boundary positions measured at half-maximal absorbance using early scans with well-defined plateaus. Diffusion experiments were performed using synthetic boundary cells at 3200 rpm. Sedimentation equilibrium experiments were performed at a rotor speed of 3200 rpm; equilibration times were 4 days. A partial specific volume of 0.736, calculated from the amino acid sequence of crm45 (*24*), was used in all calculations. For measurements in 15% sucrose, a solvent density of 1.085 g cm^{-3} was used for all calculations.

Sucrose Gradient Centrifugation. In order to separate oligomeric and monomeric species of crm45, crm45 was fractionated at pH 5.0 by sucrose gradient centrifugation. Sucrose gradients, from 10 to 30% sucrose, were poured by mixing 5.65 mL of 30% sucrose, 0.1 M citrate, 0.15 M NaCl and 5.65 mL of 10% sucrose, 0.1 M citrate, 0.15 M NaCl at pH 5.0 to a final volume of 11.3 mL. One-half milliliter of 5 mg/mL crm45 in 0.1 M citrate, pH 5.0, 0.15 M NaCl at pH 5.0 was loaded onto the top of the sucrose gradient. Crm45 at pH 5.0 was sedimented using a Beckman Model L5-75 ultracentrifuge with a SW41 swing-bucket rotor, spinning at 39 000 rpm for 5 h at 15 °C. Crm45 was then fractionated from the gradient using an an ISCO Model 185 density gradient fractionater.

RESULTS

Crm45 was expressed from *C. diphtheriae* and purified from culture filtrates at pH 7.2. After concentrating purified crm45 to 12 mg/mL, the pH dependence of crm45 solubility was determined. In 100 mM citrate buffer, 12 mg/mL, crm45 is soluble at pH 4.5 and above, and readily precipitates below pH 4.5. Although crm45 is soluble at pH 5.0, the protein can be precipitated remarkably more easily (with significantly lower concentrations of precipitating agents) than at pH 7.0. This was a preliminary indication that there may be significant structural differences in crm45 at pH 7.0 and at pH 5.0. For comparison, the pH dependence of the solubility of whole DT monomer was also determined from pH 7.0 to pH 4.0 and found to be indistinguishable from that of crm45.

Dynamic Light Scattering (DLS). In order to determine the extent of aggregation of crm45 at pH 5.0, as compared to pH 7.0, solutions of crm45 were analyzed by DLS (Table 1). At pH 7.0, DLS analysis indicates that crm45 forms a

particle with a mass of 46 kDa, corresponding to a monomer. The high polydispersity value and poor fit to a monomodal distribution indicate that although the principal scattering component of crm45 at pH 7.0 is a monomer, some aggregation does occur. An attempt to fit the data to a bimodal distribution indicates that the polydisperisity is due to a small amount of very large aggregates (data not shown). Thus, at pH 7.0, DLS indicates that crm45 is largely monomeric, with a molecular mass of 46 kDa, close to the known molecular mass of 41,826 kDa, calculated from the amino acid sequence (*24*).

At pH 5.0, DLS analysis indicates that crm45 forms a much larger particle with a mass of approximately 1100 kDa, corresponding to a high-order oligomer (see Table 1). The low polydispersity values of 8−17% and good fit to a monomodal distribution indicate that at pH 5.0 crm45 forms a uniformly sized oligomer rather than a nonhomogeneous mixture of aggregates. Similar results were obtained for crm45 at pH 4.5 and over a range of concentrations from 0.5 to 3.0 mg/mL. There was a slight trend toward higher mass estimates at higher concentrations of crm45 (see Table 1).

The mass of ∼1100 kDa estimated by DLS analysis for the crm45 oligomer at pH 5.0 can be considered to be an upper bound. If the shape of the oligomer is appreciably nonspherical, its mass may be overestimated due to a higher frictional coefficient, and hence a lower translational diffusion coefficient than for a spherical particle of the same mass. For example, DLS analysis of an IgM pentamer with a known mass of 900 kDa (*27*) resulted in a mass estimate of ∼1300 kDa (see Table 1).

In summary, DLS analysis of crm45 indicates that upon acidification from pH 7.0 to pH 5.0, crm45 undergoes a transition from a monomeric state to an oligomeric state. Since at pH 5.0 the crm45 solution is monodisperse, the low-pH oligomer is uniform in size. An upper bound for the mass of the oligomer is estimated to be approximately 1100 kDa. A crm45 oligomer of this mass would be formed by 26 subunits.

For comparison, the aggregation of whole DT monomer (which includes the R domain in addition to the C and T domains) at low pH was also characterized by DLS. Like crm45, whole DT aggregates extensively upon acidification, but at a lower pH: pH 4.5 instead of 5.0. However, for whole DT, the scattering intensity and estimated mass of the aggregates increase steadily over time. Thus, DLS analysis indicates that, in contrast to crm45, whole DT does not form a uniformly sized oligomeric species which is stable over time.

Sedimentation Studies. In order to characterize further the crm45 oligomer formed at pH 5.0, sedimentation experiments were performed in the ultracentrifuge. Sedimentation velocity analysis of crm45 at pH 5.0 reveals two boundaries (Figure 2). Approximately 25% of crm45 forms a slow moving boundary at 2.2 S, corresponding to a monomer. The other 75% of crm45 forms a fast moving boundary at approximately 22 S, corresponding to an oligomeric species.

The fast boundary exhibited significant spreading at longer time intervals, indicative of heterogeneity. Derivative analysis of the fast moving boundary results in a peak that is significantly broader than a peak calculated for an ideal species (not shown). However, the extent of boundary spreading is significantly dependent on rotor speed: the spreading of the boundary in velocity runs, measured as D_{app} (10^{-7} cm^2/s), is 30 ± 6 at a rotor speed of 56 000 rpm, but only 8 ± 1 at a speed of 24 000 rpm. Such behavior could be accounted for by a pressure dependence (*28*, *29*). If the crm45 monomer and oligomer are in equilibrium, and if the oligomer has a greater partial specific volume than the monomer, the high pressure produced inside the cell at high centrifugal force would disfavor formation of the crm45 oligomer. Thus, although significant boundary spreading is observed at high rotor speeds (high pressure), the crm45 oligomer may be homogeneous at normal pressures.

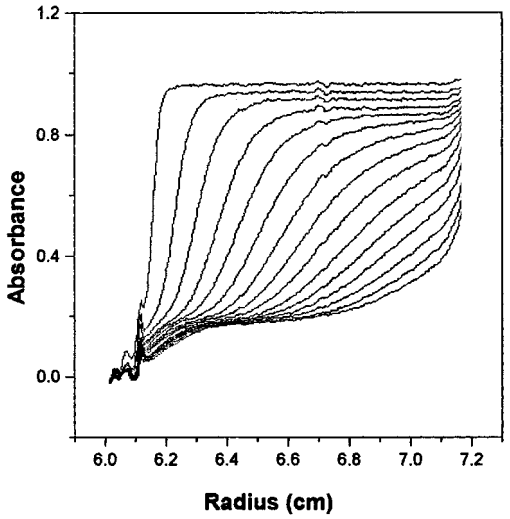

FIGURE 2: Sedimentation velocity analysis of crm45 at pH 5.0. Crm45 at 2.1 mg/mL was centrifuged at 36 000 rpm and the absorbance at 292 nm detected as a function of radial distance. Scanner tracings at successive 8 min intervals are shown superimposed. Notice that crm45 forms two boundaries: a slow moving boundary corresponding to a monomer, and a fast moving boundary corresponding to a much larger oligomer. Notice the spreading of the fast moving boundary at longer time intervals, indicative of heterogeneity. This heterogeneity could be explained by a pressure-dependent oligomerization (see text).

Table 2: Summary of Sedimentation Velocity Measurements of Crm45; These Data Show That the Size of the Crm45 Oligomer Is Independent of Its Concentration in the Range from 0.5 to 2.2 mg/mL

mg/mL	pH	$s_{20,w}$ (S)[a]	% monomer[b]
0.56	4.5	23.6 ± 0.6	26.5 ± 1.2
0.33	5.0	19.9 ± 0.1	30.5 ± 3.9
0.56	5.0	20.3 ± 0.6	25.9 ± 2.5
0.81	5.0	21.6 ± 0.3	24.9 ± 3.0
1.15	5.0	21.1 ± 0.4	21.5 ± 2.1
2.15	5.0	21.8 ± 0.4	21.1 ± 1.2

[a] Average *s*-rate of the oligomer boundary measured from runs at 24 000 rpm and 36 000 or 56 000 rpm, corrected to the standard state. [b] Measurements of all runs gave an *s*-rate for the monomer of 2.2 ± 0.4 S. The % monomer is calculated from the relative absorbance of the slow and fast moving boundaries.

In order to determine whether or not the monomeric fraction of crm45 at pH 5.0 is in equilibrium with the oligomeric fraction, sedimentation velocity experiments were performed at a range of concentrations, from 0.3 to 2.2 mg/mL (see Table 2). Over this range, the ratio of monomer to oligomer (∼1:3) does not change significantly (compare, in Table 2, % monomer at 1.2 mg/mL and at 2.2 mg/mL). This indicates that a portion of the monomeric crm45 molecules does not form the oligomer, at pH 5.0. It is conceivable that the molecules of crm45 in the monomeric fraction at

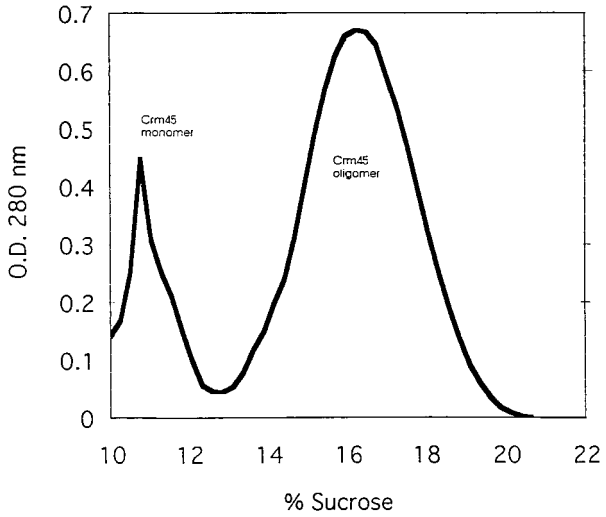

FIGURE 3: Sucrose gradient centrifugation of crm45 at pH 5.0. At pH 5.0, crm45 was sedimented at 39 000 rpm for 5 h at 15 °C through a gradient of 10−30% sucrose. The oligomeric fraction of crm45 sediments to about 15% sucrose, whereas the monomeric fraction remains at 10% sucrose.

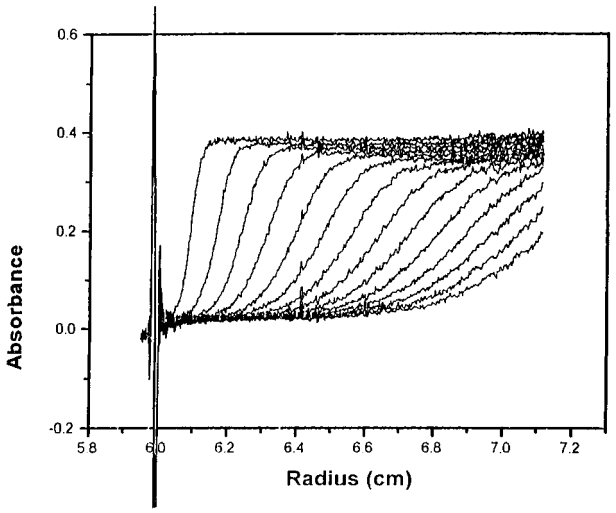

FIGURE 4: Sedimentation velocity of the sucrose-gradient purified oligomer of crm45 at pH 5.0, in 15% sucrose. 0.5 mg/mL crm45 was centrifuged at 56 000 rpm. Scanner tracings are at 8 min intervals. Notice that the monomeric fraction of crm45 has been removed (compare to Figure 2).

pH 5.0 may be chemically altered in some way such that they are unable to form the oligomer. An alternative explanation is that there is a cofactor required for formation of the oligomer, and that this cofactor is present at limiting concentrations. From the present data, it cannot be determined which of these two possible explanations (if either) is correct.

The sedimentation velocity experiments over the range of concentrations from 0.3 to 2.2 mg/mL indicate that the size of the crm45 oligomer is not dependent on concentration, since the *s*-rate of the fast-moving boundary does not show a significant concentration dependence (see Table 2). This is in contrast to the DLS analysis, which showed a slight increase in the estimated mass of the oligomer at higher concentrations.

In order to carry out further sedimentation experiments, to obtain a mass estimate for the oligomer which is independent of shape (frictional coefficient), it was necessary to separate the oligomeric fraction of crm45 from the monomeric fraction, at pH 5.0. This was accomplished by sucrose gradient sedimentation (Figure 3). A sample of 5 mg/mL crm45 was loaded onto a 10−30% sucrose gradient, and sedimented at 39 000 rpm for 5 h. As shown in Figure 3, the oligomeric portion of crm45 (∼80%) sedimented to approximately 15% sucrose, whereas the monomeric portion of crm45 remained at 10% sucrose. Thus, the oligomeric fraction of crm45 at pH 5.0 could be separated from the monomeric fraction.

After sucrose gradient purification of the crm45 oligomeric fraction at pH 5.0, sedimentation velocity of the purified oligomer was performed, in 15% sucrose (Figure 4). This resulted in only a fast moving boundary, indicating that the portion of crm45 which remains monomeric at pH 5.0 had indeed been separated. Several velocity runs at 56 000 rpm and 24 000 rpm gave an average *s*-rate of 7.3 ± 0.3 S for the crm45 oligomer at pH 5.0 in 15% sucrose.

Sucrose gradient purification of the oligomer enabled measurement of its diffusion coefficient (in 15% sucrose). This was done by forming an artificial boundary of crm45, spinning at 3500 rpm over a period of 160 min, and monitoring the spreading of the boundary due to diffusion. In this way, the diffusion coefficient of the crm45 oligomer at pH 5.0, in 15% sucrose, was determined to be 1.0×10^{-7} cm^2/s. For comparison, the diffusion coefficient of pentameric IgM (molecular mass = 900 kDa) was also determined, in 15% sucrose, and found to be 8.6×10^{-6} cm^2/s. Determination of the diffusion coefficient and sedimentation rate of crm45 at pH 5.0 in 15% sucrose resulted in a mass determination for the oligomer of 890 ± 40 kDa. This mass determination is independent of the shape of the oligomer. Thus, sedimentation velocity analysis indicates that the crm45 oligomer at pH 5.0 is formed by 20 ± 1 subunits.

After removal of the monomeric portion of crm45 at pH 5.0 by sucrose gradient sedimentation, the crm45 oligomer was analyzed by sedimentation equilibrium. The gradient formed, at equilibrium (Figure 5), is best fit by a single oligomeric species of crm45. The errors of the fit (seen above the gradient) are small and random, indicating that a single species is a reasonable fit. From four separate sedimentation equilibrium measurements, at initial concentrations of 0.2, 0.4, 0.5, and 0.9 mg/mL, the mass of the crm45 oligomer at pH 5.0 was determined to be 1000 ± 50 kDa. Initial concentrations of 0.2−0.9 mg/mL enabled measurement of the gradient at concentrations of 0.1−3.0 mg/mL. Thus, sedimentation equilibrium indicates that the crm45 oligomer at pH 5.0 is formed by 24 ± 1 subunits. This is slightly larger than the size determined by sedimentation velocity and diffusion measurements.

Size-Exclusion Chromatography. We have also attempted to characterize the oligomerization of crm45 at pH 5.0 by HPLC analytical size-exclusion chromatography (data not shown). At pH 7.0, crm45 elutes from the sizing column as a single peak at approximately 45 kDa relative to standards, corresponding to the monomer. At pH 5.0, there is no peak corresponding to the monomer. Instead crm45 elutes as a single peak just past the void volume of the column, corresponding to a very large oligomer. However, the yield obtained at pH 5.0 was less than 10% of that obtained at pH 7.0, indicating that 90% of crm45 at pH 5.0 did not elute from the column, possibly due to precipitation. When crm45 was incubated at pH 5.0 for 30 min, and then chromatographed at pH 7.0, a major peak (∼80% of the total)

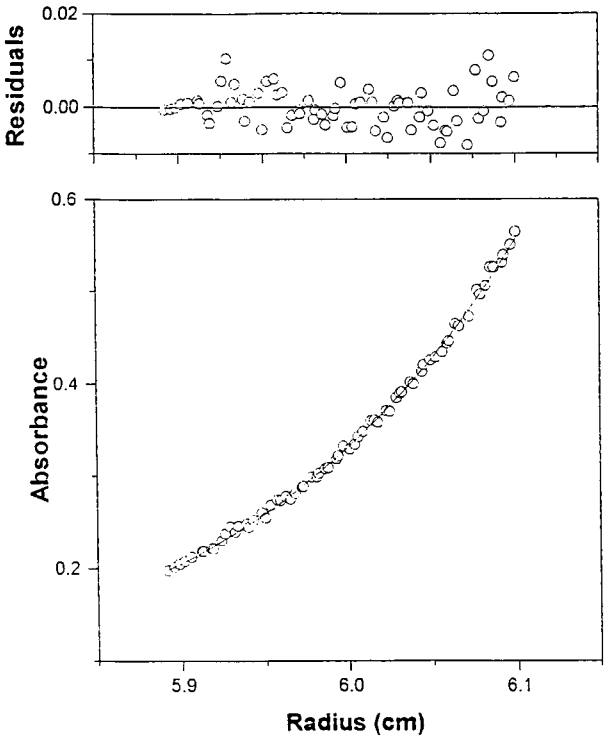

FIGURE 5: Sedimentation equilibrium analysis of crm45 at pH 5.0 in 15% sucrose. Crm45 at 0.4 mg/mL was centrifuged at 3200 rpm until equilibrium was reached (4 days). The gradient formed can be best fit to a single oligomeric species with a mass of 1005 kDa. The errors of the fit, shown above the gradient, are small and random.

corresponding to the 45 kDa monomer eluted. This experiment demonstrates that the oligomerization of crm45 at pH 5.0 is largely reversible. However, there also were peaks corresponding to slightly larger oligomers, possibly dimers and trimers, indicating that the oligomerization of crm45 is not fully reversible, at least on a time scale of ~30 min.

DISCUSSION

In this study, we have shown by (1) DLS analysis, (2) sedimentation velocity, and (3) sedimentation equilibrium, that crm45, a fragment of DT that contains the C and T domains but is missing the C-terminal R domain, forms an oligomer upon acidification from pH 7.0 to pH 5.0. From the results of these studies, it is clear that while at pH 7.0 crm45 is a monomer, at pH 5.0 crm45 is an oligomer with a mass of approximately 1000 kDa (~24 subunits).

What remains in question is the functional relevance of the crm45 oligomer formed in solution at low pH, to the membrane translocation of the C domain during the intoxication of cells by DT. Does the crm45 oligomer have a well-defined structure that functions in the membrane translocation of the C domain? Or is the oligomerization of crm45 observed in solution at pH 5.0 merely a side reaction that occurs in the absence of a lipid bilayer? If this oligomer of crm45 is relevant to membrane translocation, does whole DT, which contains the R domain, form a similar oligomer in the endosomes of host cells? Or is the proteolytic removal of the R domain required as an activation step, subsequent to receptor binding and DT internalization? In the following discussion, we address these issues.

The properties of the crm45 oligomer we have studied in solution at pH 5.0 are consistent with its possibly having a role in membrane translocation. DLS analysis results in a low polydispersity value, indicating that the oligomer is uniformly sized. This suggests that the oligomer could have a well-defined structure, and therefore possibly a function. Sedimentation equilibrium also indicates that the association of crm45 at pH 5.0 is well-defined, since the gradient is best fit by a single oligomeric species with a mass of 1000 $\pm$ 50 kDa (Figure 5). Second, according to sedimentation equilibrium analysis, the size of the oligomer is not sensitive to crm45 concentration in the range from 0.1 to 3.0 mg/mL, since measurements of the gradient at crm45 concentrations from 0.1 to 3.0 mg/mL give similar values for the mass of the oligomer.

In summary, upon acidification from pH 7.0 to pH 5.0, crm45 forms an oligomer that, according to DLS and sedimentation analyses, is uniform in size over a range of concentrations. These properties are consistent with the crm45 oligomer having a well-defined structure that could possibly be relevant to the membrane translocation of the C domain. In contrast, aggregates formed by the nonspecific association of hydrophobic surfaces that are exposed at low pH would not be expected to be uniform in size over a broad range of concentrations.

Using DLS analysis, we have observed a difference in the low-pH aggregation properties of whole DT, as compared to crm45. These two molecules differ only in that crm45 is lacking the C-terminal 149 residues which comprise the R domain. While crm45 forms a uniformly sized oligomeric species at pH 5.0 that is stable for days, whole DT forms much larger aggregates, at pH 4.5, that grow in size over the duration of the DLS experiment (~30 min). In whole DT, the presence of the R domain may lead to further associations. If the formation of the oligomer of crm45 is indeed relevant to the translocation of the C domain, these observations suggest the possibility that proteolytic removal of the C-terminal R domain (forming crm45) could be an activation step, subsequent to receptor-binding and internalization, that is necessary for the membrane translocation of the C domain.

While it is possible that the proteolytic removal of the R domain is required for translocation, there is significant evidence which suggests that such a proteolytic event may not be required as an activation step. In studies of DT intoxication of Vero cells, proteolytic intermediates of the B fragment of DT (T and C domains) were not observed prior to translocation of the C domain (*30*). In addition, it has been shown that whole DT is able to form ion-conducting channels across planar lipid bilayers, although only when the pH was lowered to below pH 5.0 (*11*). It may be that in solution, crm45 forms the oligomer more readily, without further aggregation, whereas in the endosome, where the R domain could be separated by interactions with the receptor and insertion of the T domain into the membrane, whole DT is also able to form the oligomer.

The possibility that the crm45 oligomer may be relevant to membrane translocation correlates remarkably with earlier kinetic studies of DT intoxication of Vero cells (*30, 31*). In the kinetic studies, it was observed that (1) membrane translocation of the C domain was the rate-limiting step of DT intoxication, and (2) the initial rapid rate of protein synthesis inhibition was consistent with a large constant number, or 'quantum', of C domains being released into the cytoplasm in a single event (*31*). The size of the quantum

(number of C domains entering the cytoplasm) was found to be independent of the concentration of DT added externally to the cells. From an accurate measurement of the rate of EF-2 ADP-ribosylation by the C domain under cellular conditions, and the observed rate of protein synthesis inhibition, it was estimated that approximately 20 molecules of the C domain are transferred to the cytoplasm of a cell in the quantal translocation event (*32*). This number is remarkably close to the estimated number of subunits in the crm45 oligomer characterized in this study (20−24). It was proposed that the quantal entry of C domains of DT into the cytoplasm could arise from a 'post-receptor packaging' of DT molecules in the endosome, and subsequently a destabilization of the endosomal membrane, leading to release of the endosomal contents into the cytoplasm. Alternatively, such a quantal entry of C domains into the cytoplasm leading to a rapid rate of protein synthesis inhibition could be explained by a mechanism of membrane translocation involving a ∼24 subunit oligomer of crm45 or possibly of whole DT.

The possibility that the oligomer of crm45 is relevent to membrane translocation is, however, contrary to the notion that cell killing by DT can occur by a 'one-hit' mechanism in which a single DT molecule can kill a cell. This belief is based largely on a study in which it was determined by statistical methods that a single C domain of DT can kill a cell (*33*). In this study, however, the C domain of DT was introduced into cells by artificial methods, and cell death occurred only after several hours. Thus, the forementioned study is not inconsistent with the possibility that the oligomer of crm45 is somehow involved in membrane translocation of the C domain.

In summary, the experiments presented here clearly establish that in solution, crm45, a 45 kDa fragment of DT, forms a uniformly sized, 20−24 subunit oligomer upon acidification from pH 7.0 to pH 5.0. The characteristics of the oligomer are consistent with its possibly being relevant to membrane translocation of the C domain of DT across the endosomal membrane of host cells. However, studies of crm45 oligomerization in a lipid bilayer system are needed to further validate the possible relevance of the crm45 oligomer to toxin function. At the very least, however, the solution studies presented here demonstate compelling pH-dependent oligomerization properties of crm45 which warrant further study.

ACKNOWLEDGMENT

We thank Dr. John R. Murphy for sending us the C7hm723(β-tox) M8 strain of crm45-producing *C. diphtheriae* and for useful advice concerning expression. We thank Drs. R. John Collier and Senyon Choe for useful discussions, and NIH and DOE for support.

REFERENCES

1. Montecucco, C., Papini, E., and Schiavo, G. (1994) *FEBS Lett. 346*, 92−98.
2. Higashiyama, S., Lau, K., Besner, G. E., Abraham, J. A., and Klagsbraun, M. (1992) *J. Biol. Chem. 267*, 6205−6212.
3. Morris, R. E., Gerstein, A. S., Bonventre, P. F., and Saelinger, C. B. (1985) *Infect. Immun. 50*, 721−727.
4. Blewitt, M. G., Chung, L. A., and London, E. (1985) *Biochemistry 24*, 5458−5464.
5. Sandvig, K., and Olsnes, S. (1981) *J. Biol. Chem. 256*, 9068−9076.
6. Collins, C. M., and Collier, R. J. (1987) *UCLA Symp. Mol. Cell. Biol. 45*, 41−52.
7. Zhan, H., Oh, K. J., Shin, Y. K., Hubbell, W. L., and Collier, R. J. (1995) *Biochemistry 34*, 4856−4863.
8. Hu, V. W., and Holmes, R. K. (1984) *J. Biol. Chem. 259*, 12226−12233.
9. Collier, R. J. (1975) *Bacteriol. Rev. 39*, 54−85.
10. Kagan, B. L., Finkelstein, A., and Colombini, M. (1981) *Proc. Natl. Acad. Sci. U.S.A.* 78, 4950−4954.
11. Donovan, J. J., Simon, M. I., Draper, R. K., and Montal, M. (1981) *Proc. Natl. Acad. Sci. U.S.A. 78*, 172−176.
12. Falnes, P. O., Madshus, I. H., Sandvig, K., and Olsnes, S. (1992) *J. Biol. Chem. 267*, 12284−12290.
13. Choe, S., Bennett, M. J., Fujii, G., Curmi, P. M. G., Kantardjieff, K. A., Collier, R. J., and Eisenberg, D. (1992) *Nature 357*, 216−222.
14. Bennett, M. J., and Eisenberg, D. (1994) *Protein Sci. 3*, 1464−1475.
15. Parker, M. W., Pattus, F., Tucker, A. D., and Tsernoglou, D. (1989) *Nature 337*, 93−96.
16. Muchmore, S. W., Sattler, M., Liang, H., Meadows, R. P., Harlan, J. E., Yoon, H. S., Nettesheim, D., Chang, B. S., Thompson, C. B., Wong, S.-L., Ng, S.-C., and Fesik, S. W. (1996) *Nature 381*, 335−341.
17. O'Keefe, D. O., Cabiaux, V., Choe, S., Eisenberg, D., and Collier, R. J. (1992) *Proc. Natl. Acad. Sci. U.S.A. 89*, 6202−6206.
18. Oh, K. J., Zhan, H., Cui, C., Hideg, K., Collier, R. J., and Hubbell, W. L. (1996) *Science 273*, 810−812.
19. Silverman, J. A., Mindell, J. A., Zhan, H., Finkelstein, A., and Collier, R. J. (1994) *J. Membr. Biol. 137*, 17−28.
20. Papini, E., Schiavo, G., Tomasi, M., Colombatti, M., Rappuoli, R., and Montecucco, C. (1987) *Eur. J. Biochem. 169*, 637−644.
21. Milne, J. C., Furlong, D., Hanna, P. C., Wall, J. S., and Collier, R. J. (1994) *J. Biol. Chem. 269*, 20607−20612.
22. Gouaux, J. E., Braha, O., Hobaugh, M. R., Song, L., Cheley, S., Shustak, C., and Bayley, H. (1994) *Proc. Natl. Acad. Sci. U.S.A. 91*, 12828−12831.
23. Uchida, T., Gill, D. M., and Pappernheimer, A. M., Jr. (1971) *Nature (London), New Biol. 233*, 8−11.
24. Giannini, G., Rappuoli, R., and Ratti, G. (1984) *Nucleic Acids Res. 12*, 4063−4069.
25. Mueller, J. H., and Miller, P. A. (1940) *J. Immunol. 40*, 21−32.
26. Rappuoli, R., Michel, J. L., and Murphy, J. R. (1982) *J. Bacteriol. 153*, 1202−1210.
27. Poon, P. H., Phillips, M. L., and Schumaker, V. N. (1985) *J. Biol. Chem. 260*, 9357−9365.
28. Johnson, M., and Yphantis, D. A. (1973) *Biopolymers 12*, 2477−2490.
29. Harrington, W. F., and Kegeles, G. (1973) *Methods Enzymol. 27*, 306−345.
30. Papini, E., Rappuoli, R., Murgia, M., and Montecucco, C. (1993) *J. Biol. Chem. 268*, 1567−1574.
31. Hudson, T. H., and Neville, D. M., Jr. (1985) *J. Biol. Chem. 260*, 2675−2680.
32. Hudson, T. H., and Neville, D. M., Jr. (1987) *J. Biol. Chem. 262*, 15484−15494.
33. Yamaizumi, M., Mekada, E., Uchida, T., and Okada, Y. (1978) *Cell 15*, 245−250.
34. Kraulis, P. J. (1991) *J. Appl. Crystallogr. 24*, 946−950.

BI971301X